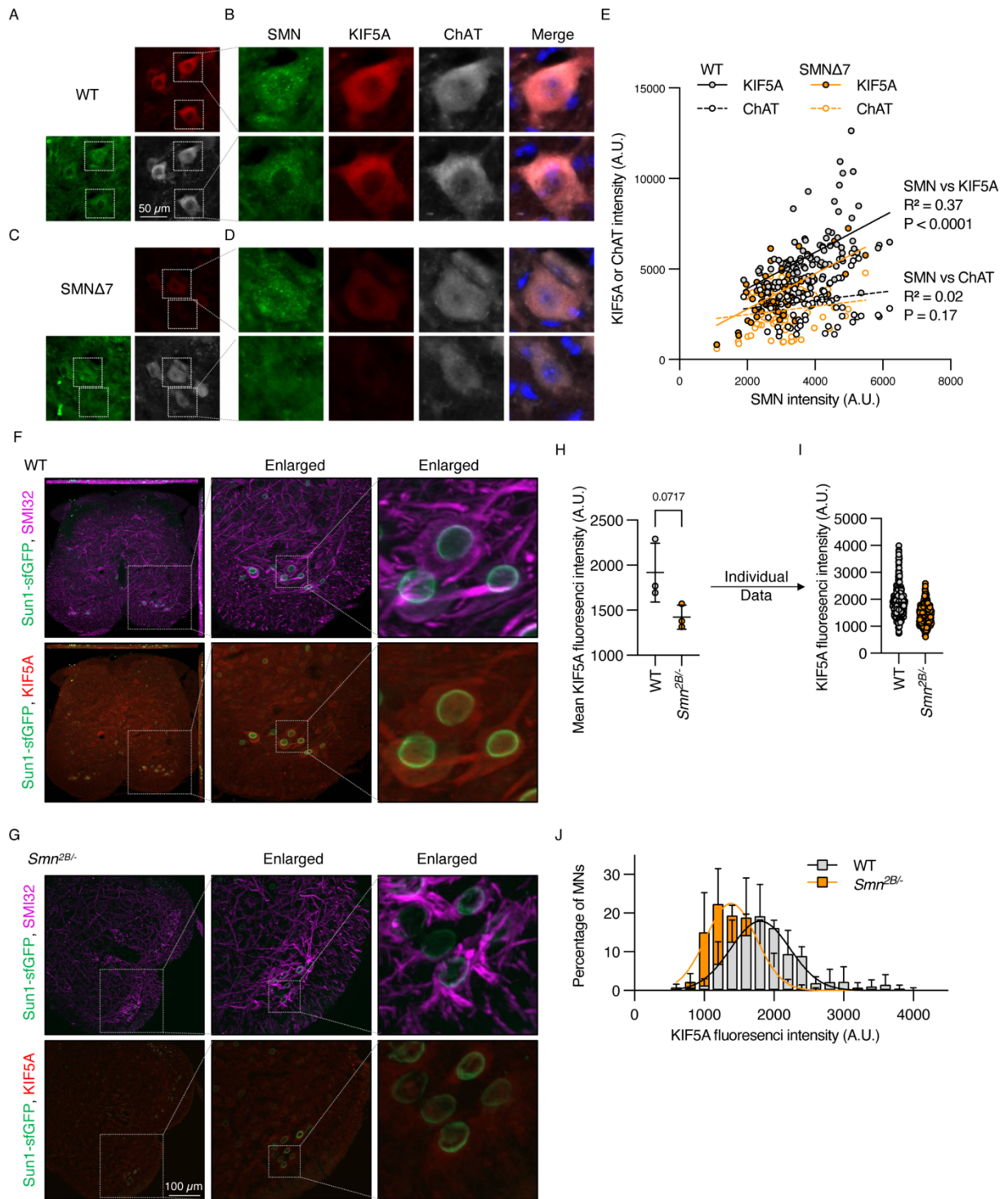


### Supplemental Figure 1. *SMN* knockdown reduces *KIF5A* expression in human neurons

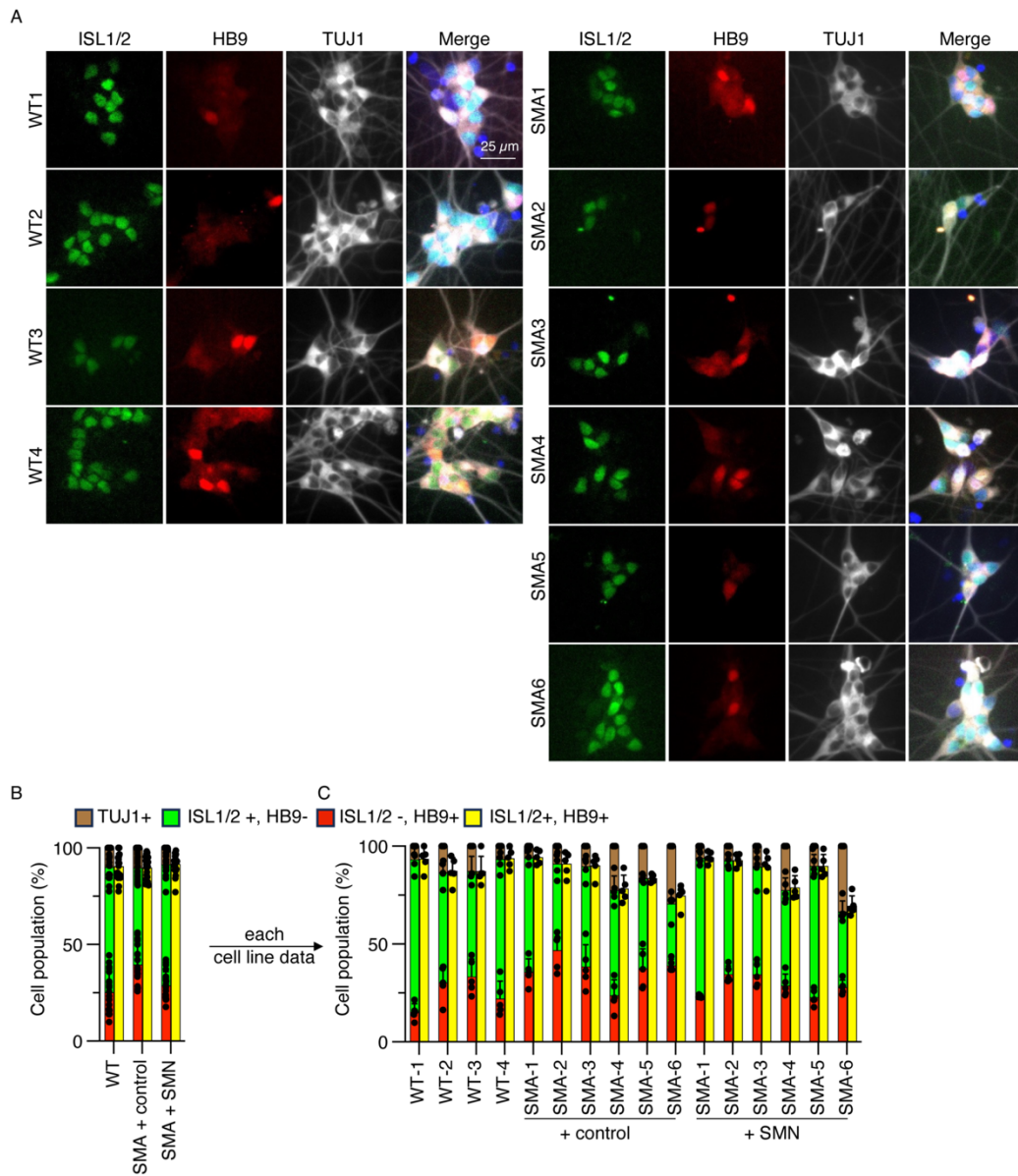
(A) RT-qPCR analysis of *i*<sup>3</sup>Neurons (*i*<sup>3</sup>Ns) following *SMN* knockdown (*SMN*-KD) showing mRNA levels of kinesin-1 family members (*KIF5A*, *KIF5B*, and *KIF5C*) and *ACAT2*. Both *KIF5A* and *ACAT2* mRNA levels were reduced compared with SCR *i*<sup>3</sup>N. (B) Immunoblot analysis of *i*<sup>3</sup>Ns lysates following *SMN*-KD showing reduced *SMN* and *KIF5A* protein levels, whereas *KIF5B*, *KIF5C*, and *ACAT2* protein levels remained unchanged. To achieve a mild KD, doxycycline was used at 0.5  $\mu$ g/ml (standard concentration = 2  $\mu$ g/ml). Dashed lines indicate that lanes were derived

from different membranes. **(C)** Quantification of immunoblot data shown in **(B)**. SMN and KIF5A protein levels were significantly reduced in *SMN*-KD i<sup>3</sup>Ns relative to SCR controls, whereas ACAT2 protein levels were not altered. Data represent three independent experiments. Statistical analysis was performed using an unpaired two-tailed t-test with Welch's correction. **(D–F)** *SMN*-KD preferentially reduces KIF5A expression in healthy donor-derived motor neurons (iMNs). Motor neurons differentiated from four healthy donor iPSC lines were analyzed (see Supplemental Table 1 for cell line details). **(D)** RT-qPCR analysis of iMNs following *SMN*-KD showing a preferential reduction of KIF5A mRNA compared with other kinesin-1 family members. **(E and F)** Immunoblot analysis and quantification of protein levels in iMNs following *SMN*-KD, demonstrating limited or context-dependent changes compared with the robust reduction observed for KIF5A. **(G–I)** Single-molecule fluorescence in situ hybridization (smFISH) analysis of KIF5A mRNA in SCR and *SMN*-KD i<sup>3</sup>Ns. Representative images from SCR i<sup>3</sup>Ns **(G)** and *SMN*-KD i<sup>3</sup>Ns **(H)**, and quantification of KIF5A mRNA puncta per cell **(I)** demonstrate a reduction of KIF5A transcripts following *SMN*-KD. Statistical analysis was performed using an unpaired two-tailed t-test with Welch's correction (n = 5).



**Supplemental Figure 2. KIF5A expression correlates with SMN levels in spinal motor neurons of SMA mouse models**

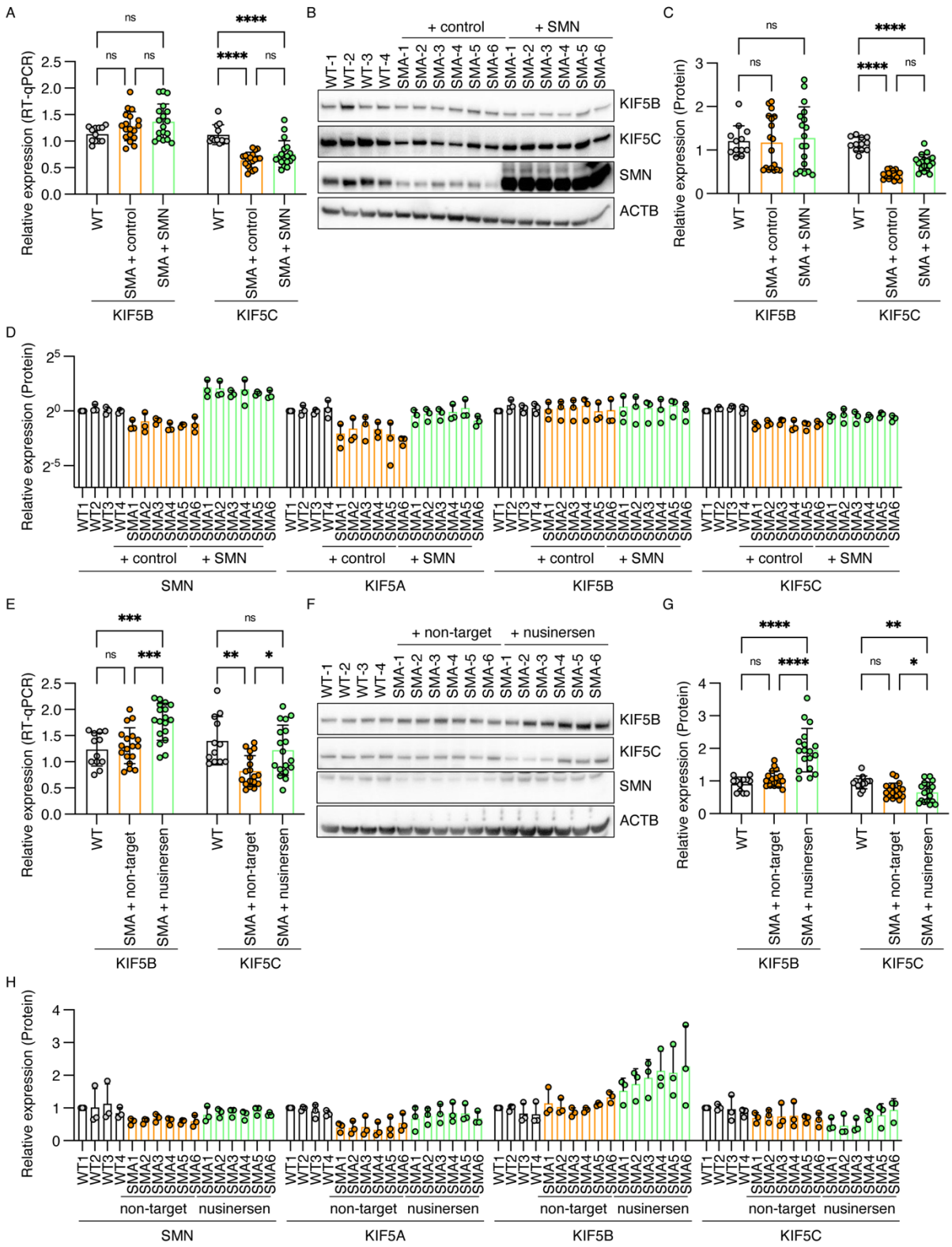
(A–D) Representative immunofluorescence images of lumbar spinal cord sections stained for SMN, KIF5A, and the motor neuron marker ChAT from postnatal day 10 (P10) age-matched control mice (A and B) and SMN $\Delta$ 7 mice (C and D). Spinal motor neurons in SMN $\Delta$ 7 mice exhibited reduced KIF5A expression compared with controls. (B) Higher-magnification images of representative motor neurons from control mice indicated in (A). (D) Higher-magnification images of representative motor neurons from SMN $\Delta$ 7 mice indicated in (C), including examples retaining detectable SMN and KIF5A expression. (E) Correlation analysis between SMN and KIF5A fluorescence intensities in individual motor neurons from SMN $\Delta$ 7 mice, revealing a positive correlation. No such correlation was observed between ChAT and SMN intensities. (F–J) KIF5A expression in a milder SMA mouse model. (F and G) Representative immunofluorescence images of lumbar spinal motor neurons from postnatal day 17 (P17) *Smn*<sup>2B/-</sup> mice (G) and corresponding control mice (F). Motor neuron nuclei were genetically labeled with Sun1-sfGFP (green). Neuronal identity was confirmed by SMI32 immunostaining (Top panel, purple), and KIF5A expression was visualized by immunostaining (bottom panel, red). (H) Quantification of KIF5A fluorescence intensity in spinal motor neurons from *Smn*<sup>2B/-</sup> mice, showing a trend toward reduced KIF5A expression compared with controls. (I) Individual motor neuron KIF5A intensity values corresponding to the quantification shown in (H). (J) Frequency distribution analysis of KIF5A fluorescence intensity across both SMA mouse models, showing a shift toward lower KIF5A intensity values in *Smn*<sup>2B/-</sup> mice.



**Supplemental Figure 3. Motor neuron differentiation efficiency is consistent across all iPSC lines.**

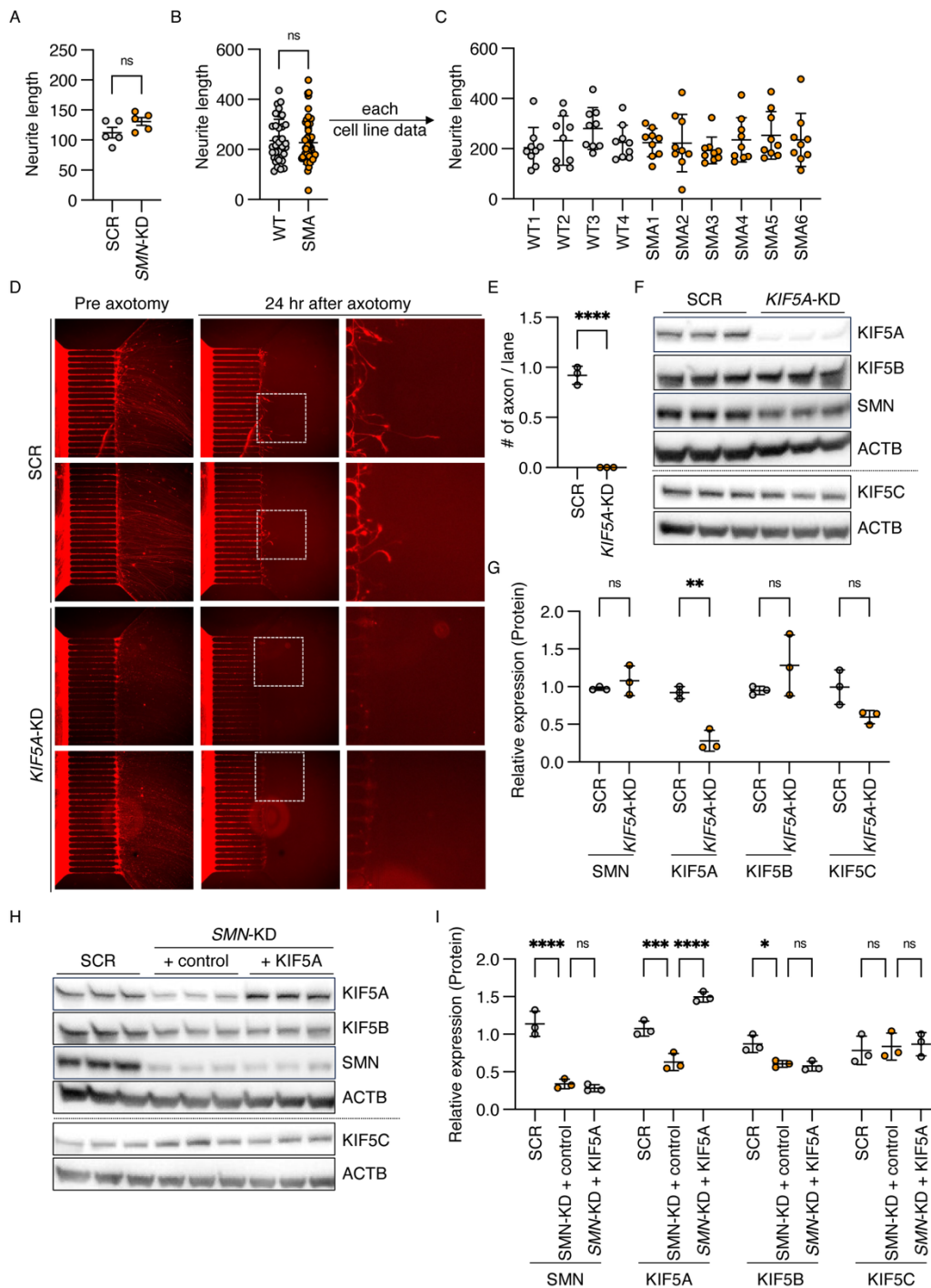
To confirm comparable motor neuron differentiation efficiency between wild-type (WT) and SMA iPSC lines, immunostaining was performed at day 20 of differentiation. **(A)** Representative immunofluorescence images of iPSC-derived motor neurons at day 20 stained for  $\beta$ III-tubulin (TUJ1), HB9 (red), and ISL1/2 (green), both of which are motor neuron-specific markers. **(B)** and

C) Quantification of motor neuron induction efficiency using the ImageXpress system. Five regions per sample were imaged, and five biologically independent samples were analyzed. **(B)** Group-averaged data are shown for WT, SMA + control, and SMA + SMN conditions. **(C)** Data from individual iPSC lines are shown. In the bar graphs, brown indicates the total population of TUJ1-positive nuclei (set to 100%). Red and green indicate nuclei positive for HB9 or ISL1/2 alone, respectively, while yellow represents nuclei positive for either HB9 or ISL1/2. Statistical analysis was performed using one-way ANOVA on group-aggregated values (WT, SMA + control, and SMA + SMN) for TUJ1-positive, HB9-positive, ISL1/2-positive, and HB9+ISL1/2-positive nuclei. No significant differences were observed among groups, indicating comparable motor neuron differentiation efficiency across all iPSC lines.



**Supplemental Figure 4. Expression of kinesin-1 family members following SMN restoration in SMA patient-derived motor neurons**

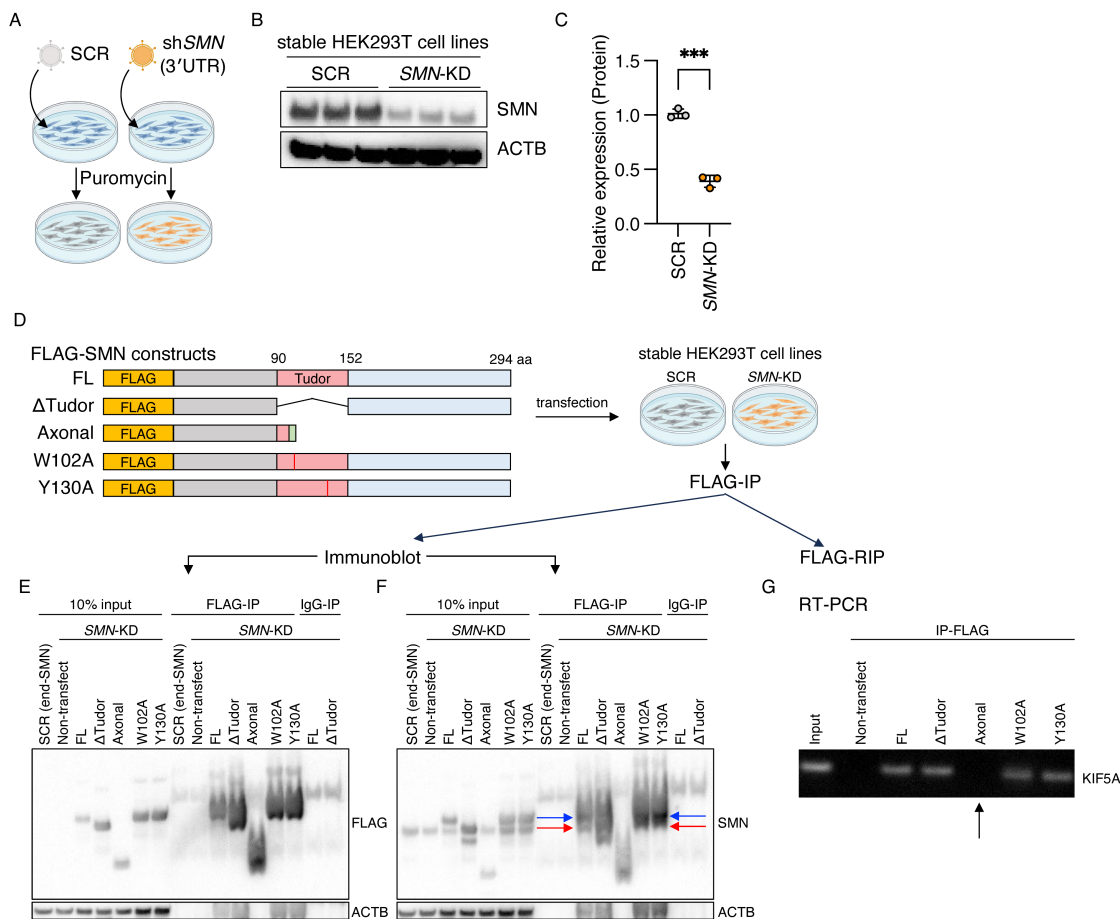
(A–D) Analysis of kinesin-1 family expression following SMN overexpression in SMA patient–derived motor neurons (iMNs). (A) RT-qPCR analysis of KIF5B and KIF5C mRNA levels in WT, SMA + control lentivirus, and SMA + SMN overexpression conditions. (B) Representative immunoblots showing protein levels of KIF5B and KIF5C under the same conditions. SMN and ACTB bands from Figure 3E are shown from the same membrane. (C) Quantification of immunoblot data shown in (B), indicating limited or context-dependent effects of SMN overexpression on KIF5B and KIF5C protein levels, relative to the restoration of KIF5A shown in Figure 3. (D) Individual immunoblot data for each cell line, showing protein levels of SMN, KIF5A, KIF5B, and KIF5C under WT, SMA + control, and SMA + SMN overexpression conditions. These data correspond to the group-averaged quantifications shown in Figure 3F and Supplemental Figure 4C. (E–H) Analysis of kinesin-1 family expression following nusinersen treatment in SMA patient-derived iMNs. (E) RT-qPCR analysis of KIF5B and KIF5C mRNA levels in WT, SMA + non-targeting ASO, and SMA + nusinersen conditions. (F) Representative immunoblots showing protein levels of KIF5B and KIF5C following ASO treatment. (G) Quantification of immunoblot data shown in (F), indicating no consistent restoration of KIF5B or KIF5C protein levels following nusinersen treatment. (H) Individual immunoblot data for each iPSC line, including SMN and KIF5A (corresponding to Figure 3I) as well as KIF5B and KIF5C, across WT, SMA + non-targeting ASO, and SMA + nusinersen conditions. These data correspond to the group-averaged quantifications shown in Figure 3I and Supplemental Figure 4G. Quantified data in (A,C,E, and G) were derived from three biologically independent experiments performed in triplicate and analyzed using one-way ANOVA followed by Tukey’s multiple comparisons test.



### Supplemental Figure 5. KIF5A regulates axonal regeneration in *i*<sup>3</sup>Neurons

(A–C) Neurite length is not significantly altered by *SMN* knockdown (*SMN*-KD) in *i*<sup>3</sup>Neurons (*i*<sup>3</sup>Ns) or under SMA conditions. Neurite length (µm/cell) shows no significant differences in *SMN*-

KD i<sup>3</sup>Ns or SMA patient derived motor neurons (iMNs) compared with controls (scrambled shRNA; SCR for i<sup>3</sup>Ns (A) or WT for iMNs (B)). Cell line-specific data corresponding to (B) are shown in (C). (D–G) *KIF5A*-KD impairs axonal regeneration independently of other kinesin-1 family members. (D) Representative live-cell images of i<sup>3</sup>Ns cultured in microfluidic devices before and after axonal transection. Axons extend from the somatic compartment (left) into the axonal compartment (right). The length of each microchannel is 450 μm. (E) Quantification of regenerating axons per microfluidic channel following *KIF5A*-KD. Data represent the average number of regenerating axons per channel, normalized to control conditions (n = 3 independent experiments, with 2 images per experiment; 17–20 channels per image; >100 channels total). Statistical analysis was performed using an unpaired two-tailed t-test with Welch's correction. (F and G) Immunoblot analysis confirming efficient *KIF5A*-KD in i<sup>3</sup>Ns following 10 days of shRNA induction and demonstrating that *KIF5A*-KD does not alter the protein levels of other kinesin-1 family members. Representative immunoblots are shown in (F). Dashed lines indicate that lanes were derived from different membranes. Quantification is shown in (G). Data represent three independent experiments. Statistical analysis was performed using an unpaired two-tailed t-test with Welch's correction. (H and I) Immunoblot analysis confirming *KIF5A* overexpression in *SMN*-KD i<sup>3</sup>Ns, corresponding to experiments shown in Figure 4. Representative immunoblots are shown in (H). Dashed lines indicate that lanes were derived from different membranes. Quantification is shown in (I). Statistical analysis was performed using one-way ANOVA followed by Tukey's multiple comparisons test.



### Supplemental Figure 6. Characterization of SMN–*KIF5A* mRNA association using SMN domain mutants

(A–C) Generation and validation of stable *SMN*-knockdown (KD) HEK293T cells used for luciferase reporter (Figure 5, C and D) and RNA immunoprecipitation (RIP) assays (panel D–F). (A) Experimental schematic. (B) Immunoblot results confirming efficient *SMN*-KD following lentiviral transduction and puromycin selection. (C) Quantification of SMN protein levels relative to control cells. Statistical analysis was performed using an unpaired two-tailed t-test with Welch’s correction. (D–G) RIP assays using FLAG-tagged SMN constructs carrying Tudor domain deletions or point mutations (W102A and Y130A), as well as axon-SMN. (D) Experimental schematic of RIP assays using FLAG-tagged SMN constructs. (E) Immunoblot analysis of FLAG

immunoprecipitates detected with an anti-FLAG antibody, confirming efficient expression and immunoprecipitation of FLAG-tagged SMN constructs. Endogenous SMN is not detected in FLAG immunoblots. (F) Immunoblot analysis of the same FLAG immunoprecipitates detected with an anti-SMN antibody. Both FLAG-tagged SMN (blue arrow) and endogenous SMN (red arrow) are detected, indicating co-immunoprecipitation of endogenous SMN with FLAG-tagged constructs, except for axon-SMN. (G) RIP followed by RT-PCR analysis assessing association of SMN constructs with KIF5A mRNA. Truncated axonal SMN constructs failed to associate with KIF5A mRNA (black arrow in G), whereas Tudor domain-deficient or mutant SMN constructs retained detectable association. This residual association is likely mediated by co-immunoprecipitated endogenous wild-type SMN, which remains capable of binding KIF5A mRNA.

### **List of Supplemental Tables**

Supplemental Table 1: Stem cell information

Supplemental Table 2: DEGs lists

Supplemental Table 3: Medium list

Supplemental Table 4: Antibodies list

Supplemental Table 5: Primers